Higher Order Ionospheric Correction in Radio Occultation Inversion

Mohammed Mainul Hoque

Abstract – Global navigation satellite system (GNSS) radio occultation (RO) signals are commonly used to retrieve vertical electron density profile. However, GNSS RO signals are strongly affected by ionospheric refraction because they travel long ionospheric limb paths. Our investigation using a simulation study shows that RO electron density retrieval improves after applying higher order ionospheric corrections that are not generally considered. Depending on profile shapes, the improvement varies from about 3% to 25% for electron density estimation along altitudes. We found that the percentage improvement is greater at lower and higher altitudes than at the peak electron density height.

1. Introduction

Global navigation satellite system (GNSS) signals are strongly affected by ionospheric refraction during radio occultation (RO) due to long ionospheric travel paths. Inhomogeneous plasma distribution and anisotropy cause higher order nonlinear refraction effects on GNSS signals [1, 2]. However, nonlinear terms such as the second and third order ionospheric terms and ray path bending effects are not generally considered when computing total electron content (TEC) through a linear combination of dual-frequency phase observables. The TECs are used to reconstruct the electron density profile along the altitude by using an inversion technique known as *onion peeling* [3]. However, the accuracy of the inversion technique can be improved if the higher order terms are corrected for. In [4], it is shown that bending and dispersion may cause a systematic residual error of up to 20 TECU (1 TECU $= 10^{16}$ electron/m^2) in RO TEC estimation by using a dual-frequency geometry-free combination. Using both frequencies, as well as precise orbit information, the proposed combination could eliminate the bending term and leave only a geomagnetic field–related term as the main residual. Using a simulation study, we have investigated the second-order term in the refractive index and effects due to the straight line of sight (LOS) propagation assumption, such as the excess path length of the signal, in addition to the LOS path and the TEC difference between the curved path and the LOS path for selected GPS–COSMIC/FORMOSAT-3 occultation events.

Manuscript received 23 December 2021.

Mohammed Mainul Hoque is with the German Aerospace Center, Kalkhorstweg 53, 17235 Neustrelitz, Germany; e-mail: mainul.hoque@dlr.de.

2. Higher Order Ionospheric Terms

The dual-frequency TEC along straight LOS path $\mathrm{TEC}_{\mathrm{LOS}}$ can be written for the carrier phase difference and higher order ionospheric terms as [1]

$$\mathrm{TEC}_{\mathrm{LOS}} = \frac{2f_1^2 f_2^2(\Phi_1 - \Phi_2)}{K\left(f_1^2 - f_2^2\right)} - \Delta\mathrm{TEC}_{\mathrm{bend}} - \Delta\mathrm{TEC}_{\mathrm{second}} + \Delta\mathrm{TEC}_{\mathrm{len}} \tag{1}$$

in which

$$\Delta\mathrm{TEC}_{\mathrm{bend}} = \frac{f_1^2\Delta\mathrm{TEC}_{\mathrm{bend2}} - f_2^2\Delta\mathrm{TEC}_{\mathrm{bend1}}}{\left(f_1^2 - f_2^2\right)} \tag{2}$$

$$\Delta\mathrm{TEC}_{\mathrm{second}} = \frac{q}{K}\frac{f_1^2 + f_1 f_2 + f_2^2}{f_1 f_2 (f_1 + f_2)} \tag{3}$$

$$\Delta\mathrm{TEC}_{\mathrm{len}} = \frac{2}{K}\frac{f_1^2 f_2^2 (d_{\mathrm{len2}} - d_{\mathrm{len1}})}{\left(f_1^2 + f_2^2\right)} \tag{4}$$

$$q = 2.2566 \times 10^{12} \int n_e B \cos\Theta ds \tag{5}$$

where $K = 80.6$, Φ_1 and Φ_1 are the carrier phases measured at GNSS f_1 and f_2 frequency, n_e is the electron density along ray path s, B is the geomagnetic induction, and Θ is the angle between the ray direction and magnetic field vector. The quantities $\Delta\mathrm{TEC}_{\mathrm{bend1}}$ and $\Delta\mathrm{TEC}_{\mathrm{bend2}}$ are the physical TEC differences between the LOS ray and the true curved ray correspond to f_1 and f_2 signals, respectively. Similarly, d_{len1} and d_{len2} denote the excess path length in addition to the LOS path length. The quantity $\Delta\mathrm{TEC}_{\mathrm{second}}$ is the second-order term, and $\Delta\mathrm{TEC}_{\mathrm{len}}$ and $\Delta\mathrm{TEC}_{\mathrm{bend}}$ are the bending-related higher order terms in the dual-frequency TEC estimation. All these terms have been plotted as a function of tangential height in Figures 4 and 5 for Case 1 and 2 electron density profiles (see Figure 1). For the ray tracing computation, the ionosphere is assumed to be composed of numerous thin spherical layers in which the medium is homogeneous. The ray path geometry is taken from a typical GPS–COSMIC/FORMOSAT-3 occultation event.

Figure 2 shows that the electron density *N*e distribution along range (COSMIC to GPS direction) varies significantly, depending on the ray path geometry (i.e., tangential height). Tangential height is defined as the minimum height of the ray path from the Earth's surface. At a lower tangential height (e.g., 100 km), the

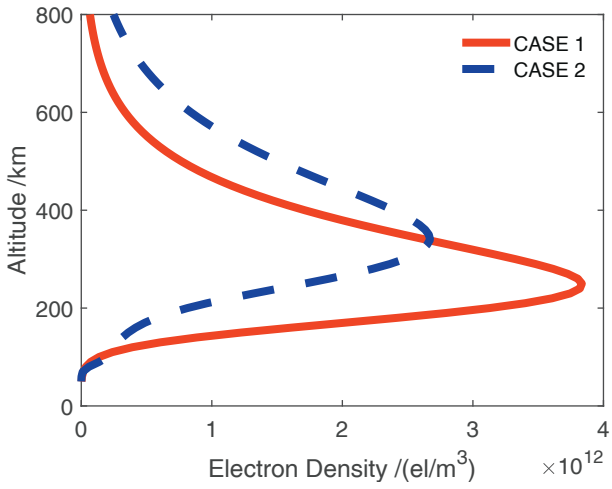

Figure 1. Case 1 and 2 electron density profiles generated by using three Chapman layers with vertical TEC (VTEC) = 100 TECU (1 TECU = 10^{16} electron/m^2). Case 2 was a thick profile (blue curve), with a relatively smaller peak density and larger scale height (profile thickness), whereas Case 1 was a thin profile, having higher peak density and smaller scale height.

*N*e distribution shows two peaks, whereas a ray path with tangential height near the peak density height shows a single peak in the *N*e distribution. The reason is that the ray path with low tangential height crosses the ionospheric F layer (>140 km) two times before and after traveling through the D and E layer (50 km to 140 km).

Figure 3 shows variation of ray path deviation from the LOS path computed by using a two-dimensional (2D) ray tracing tool [2]. Note that ray paths with high tangential height travel below the LOS path, with respect to the Earth's surface, and are represented by negative ray path deviations. The magnitude of ray path deviation varies, depending on the elevation angle and refractive index profile obtained from the *N*e distribution.

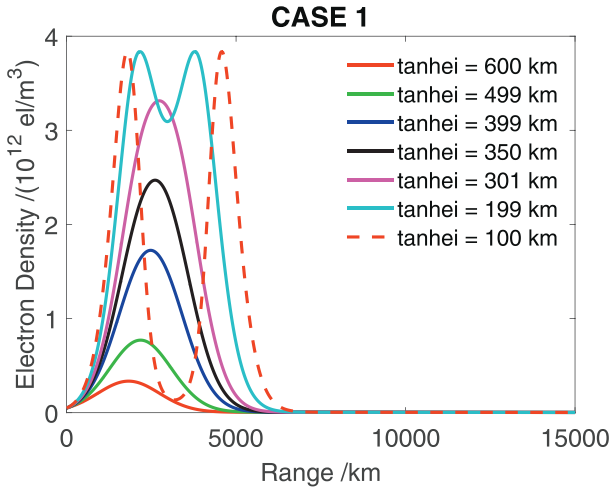

Figure 2. Electron density variation along range for ray paths having a different tangential height for Case 1. Case 2 had a similar variation with reduced magnitude.

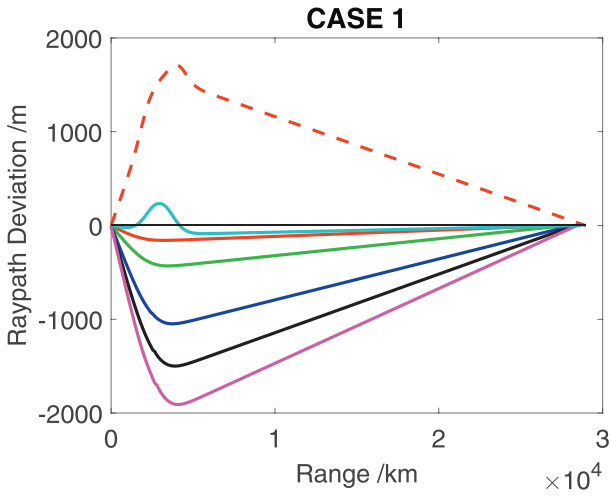

Figure 3. Variation of ray path deviation from the LOS propagation for Case 1. Similar to Figure 2, each color represented a ray path with a different tangential height.

Figures 4 and 5 show the variation of higher order ionospheric terms due to the second-order term in the refractive index and effects due to ray path bending errors or curvature effects for Case 1 and 2 profiles. The 2D ray tracing tool [2] is used to trace rays for GPS–COSMIC RO paths, where the background ionization is given by Case 1 and 2 electron profiles. The background magnetic field is given by the International Geomagnetic Reference Field model. The abovementioned higher terms are obtained as outputs of the ray tracing tool. We found that the higher order terms are larger for a thin profile than those for a thick profile. The magnitude of ΔTEC_{bend} is found to be larger than for ΔTEC_{len}, and the second-order term is very small compared with the bending-related errors. Because the

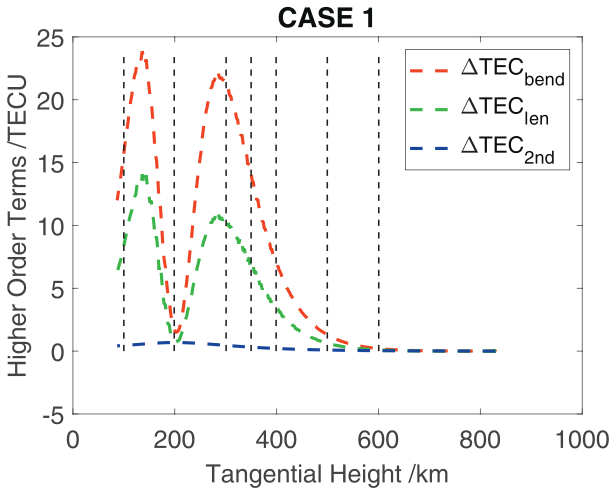

Figure 4. Variation of higher order ionospheric terms in RO TEC estimation as a function of tangential height for Case 1.

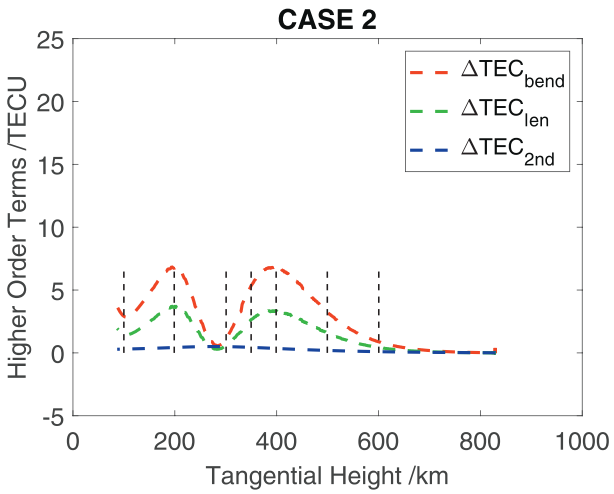

Figure 5. Variation of higher order ionospheric terms in RO TEC estimation as a function of tangential height for Case 2.

terms ΔTEC_{bend} and ΔTEC_{len} are opposite in sign in (1), some effects are canceled out, indicating that both terms need to be simultaneously considered. The results are in consistent with the results found for ground reception [5]. In Figures 4 and 5, each vertical dashed line represents a different tangential height considered in Figure 2.

3. RO Inversion Results

We computed TEC along LOS and along curvature paths by using the ray tracing tool for Cases 1 and 2. In addition, higher order terms, such as the second-order term, excess TEC and excess path and phase terms, are estimated. A model-assisted RO inversion method [3] is applied to the slant TEC (sTEC) data. The method uses spherical symmetry and the onion peeling technique for estimating electron

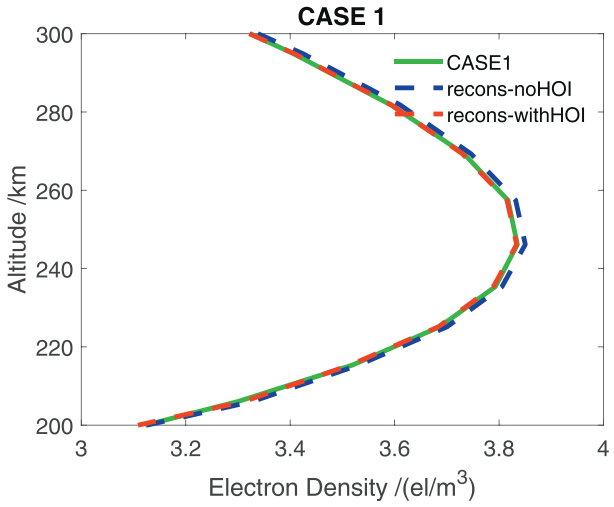

Figure 6. RO retrieval with (leveled as recons-withHOI) and without (leveled as recons-noHOI) higher order corrections for Case 1.

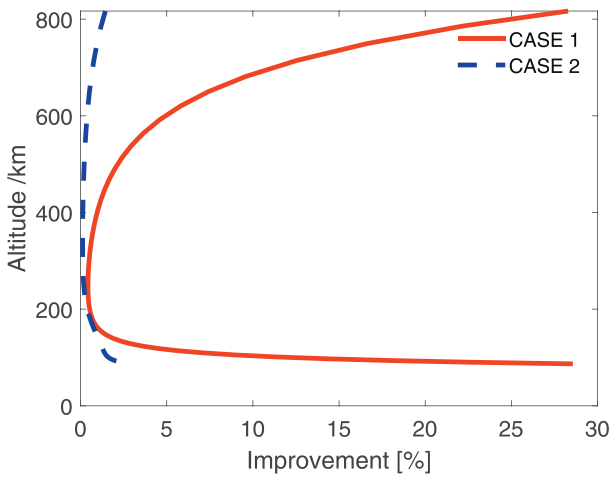

Figure 7. Percentage improvement in RO retrieval after applying higher order correction.

density from the top to bottom RO height. On the basis of the input sTEC data, we retrieved electron density profiles with the corrected data of the higher order terms (i.e., TEC_{LOS}) and without correction data (i.e., $TEC_{LOS} + \Delta TEC_{bend} - \Delta TEC_{len} + \Delta TEC_{second}$). The retrieved electron density profiles are plotted in Figure 6 for Case 1. The green-colored plot shows the original Case 1 profile, whereas the red- and blue-colored plots show the RO retrieval with and without higher order corrections. We find that the red plot is closer to the truth.

We computed the percentage inversion error for the original Case 1 and 2 profiles by (6) and (7). The improvement is determined by (8). The variations of percentage improvement along height are plotted in Figure 7.

$$\text{inversion\_error}_{\text{noHOIcorr}} = \frac{\left(Ne_{\text{noHOIcorr}} - Ne_{\text{Case1,2}}\right) \times 100\%}{Ne_{\text{Case1,2}}} \quad (6)$$

$$\text{inversion\_error}_{\text{withHOIcorr}} = \frac{\left(Ne_{\text{withHOIcorr}} - Ne_{\text{Case1,2}}\right) \times 100\%}{Ne_{\text{Case1,2}}} \quad (7)$$

$$\text{improvemen}[\%] = \text{inversion\_error}_{\text{noHOIcorr}} - \text{inversion\_error}_{\text{withHOIcorr}} \quad (8)$$

Figure 7 shows that RO inversion improves after applying the higher order corrections. Depending on profile shapes the improvement varies from 3% to 25% for an electron density profile having a TEC of 100 TECU. The improvement is greater for the Case 1 profile, as expected. We found that percentage improvement is greater at higher and lower altitudes compared with that at peak electron density height. The model-assisted RO inversion method uses differential sTEC measurements derived from carrier phase only

data; thus, the common ambiguity, satellite and receiver bias, and clock terms are already removed. However, assumption of spherical symmetry may cause significant errors, especially during gradient conditions. Using simulation studies, [6] found that the errors in RO electron density retrieval due to spherical symmetry assumption might exceed 50% below the E-layer height ($<$140 km), whereas the errors were found below 20% at the peak density height.

Our investigation shows that the accuracy of the RO inversion will be improved if higher order ionospheric corrections are applied. However, more investigations are required considering real measurements. The errors caused by spherical symmetry assumption may exceed the higher order effects in practical cases.

Note that in practical cases, we need knowledge of the background electron density for correcting higher order terms that is not available. However, an electron density profile retrieved in a first iteration without higher order corrections can be used, together with a ray tracing tool, to compute and correct the higher order terms. It is assumed that the generated profile in a second iteration will be higher order errors corrected one.

4. Conclusions

By simulation study, it has been shown that GNSS RO observations are strongly affected by ionospheric refraction. The higher ionospheric propagation effects due to geomagnetic induction and ray path bending are computed by using ray tracing simulation. The impact of these higher order terms on RO inversion is derived. The impact is found relatively higher for a thin profile compared with a thick profile. When the higher order corrections are applied, we find that the improvement varies from about 3% to 25%, depending on the tangential height of the ray path. We found that the percentage improvement is greater at lower and higher altitudes than at the peak electron density height.

5. References

1. M. M. Hoque and N. Jakowski, “Higher Order Ionospheric Propagation Effects on GPS Radio Occultation Signals,” *Advances in Space Research*, **46**, 2, July 2010, pp. 162-173, doi: 10.1016/j.asr.2010.02.013.
2. M. M. Hoque and N. Jakowski, “Estimate of Higher Order Ionospheric Errors in GNSS Positioning,” *Radio Science*, **43**, 5, October 2008, doi: 10.1029/2007RS003817.
3. N. Jakowski, A. Wehrenpfennig, S. Heise, C. Reigber, H. Lühr, et al., GPS Radio Occultation Measurements of the Ionosphere from CHAMP: Early Results,” *Geophysical Research Letters*, **29**, 10, May 2002, pp. 95-1-95-4, doi: 10.1029/2001GL014364.
4. S. Syndergaard, A New Algorithm for Retrieving GPS Radio Occultation Total Electron Content, *Geophysical Research Letters*, **29,** 16, August 2002, pp. 55-1-55-4, doi: 10.1029/2001GL014478.
5. M. M. Hoque and N. Jakowski, “New Correction Approaches for Mitigating Ionospheric Higher Order Effects in GNSS Applications,” 25th International Technical Meeting of the Satellite Division of the Institute of Navigation, Nashville, TN, USA, September 17–21, 2012, pp. 3444-3453.
6. M. Hernández-Pajares, J. M. Juan, and J. Sanz, Improving the Abel Inversion by Adding Ground GPS Data to LEO Radio Occultations in Ionospheric Sounding, *Geophysical Research Letters*, **27**, 16, August 2000, pp. 2473-2476.